

GIS Mapping of Tsunami Vulnerability: Case Study of the Jembrana Regency in Bali, Indonesia

Tumpal P. T. Sinaga*, Adhi Nugroho**, Yang-Won Lee***, and Yongcheol Suh****

Received November 30, 2008/Revised December 13, 2009/Accepted June 15, 2010

Abstract

The coastal zone is a precious area that sustains many people and various ecosystems of high biological and economic importance. However, ecosystems and human settlements in coastal regions can be vulnerable to natural disasters such as tsunamis. Around Indonesia, seismic activity under the Indian Ocean has caused frequent earthquakes and tsunamis. In this paper, we describe a GIS-based multi-criteria analysis of tsunami vulnerability for the Jembrana Regency in Bali, Indonesia. We used multiple geospatial variables of topographic elevation and slope, topographic relation to tsunami direction, coastal proximity, and coastal shape. We also incorporated expert knowledge by the Analytic Hierarchy Process (AHP) to construct a weighting scheme for the geospatial variables. In order to examine tsunami vulnerability in relation to land use, we overlaid an official land-use map on the tsunami vulnerability map. Buildings as well as residential and agricultural areas were found to be particularly at risk in our study area. GIS-based analyses can aid in a wide range of disaster assessment and facilitate regional planning for management and mitigation of natural disasters such as tsunamis. We expect that the tsunami vulnerability map presented here will contribute to preliminary tsunami mitigation and management efforts in the Jembrana Regency.

Keywords: *GIS, land use, multi-criteria analysis, tsunami vulnerability*

1. Introduction

Coastal regions make up only 4% of the world's land area but are home to one third of the world's population. According to the *United Nations Environment Programme (UNEP) World Conservation Monitoring Centre (2006)*, the coastal population may double in 15 years. In addition to human populations, the coastal zone also supports a variety of ecosystems of high biological and economic importance, including coral reefs, lagoons, sea-grass beds, sand dunes, mangrove forests, and other coastal vegetation. However, ecosystems and human settlements in coastal regions can be vulnerable to natural disasters such as tsunamis.

Indonesia suffers from frequent earthquakes and tsunamis caused by seismic activity under the Indian Ocean. In recent 380 years between 1629 and 2009, 316 significant earthquakes have occurred in Indonesia (<http://www.ngdc.noaa.gov/hazard/earthqk.shtml>). Most of tsunami occurrences in Indonesia have been caused by tectonic earthquakes along subduction and active seismic zones. Fig. 1 shows a seismic hazard map of Indonesia, indicating earthquake risk in large parts of Sumatra and Java. Using historical records, Diposaptono and Budiman (2005)

distinguished 89 tsunami-vulnerable areas distributed throughout all areas of the Indonesian islands. A wide range of coastal areas were estimated to be vulnerable to tsunami hazards, including western Sumatra, southern Java, southern Bali, southern Sumbawa, northern and southern Flores, the Maluku archipelago, northern and southern Papua, and northern Sulawesi.

A number of studies have examined the 2004 Indian Ocean tsunami, which originated near Sumatra. These studies included examinations of tsunami propagation models (Jaffe and Gelfenbuam, 2007; Roy *et al.*, 2007; Koh *et al.*, 2009; Wijetunge, 2009), geomorphologic changes caused by the tsunami (Srinivasalu *et al.*, 2007; Paris *et al.*, 2007; Fagherazzi and Du, 2008; Yan and Tang; 2009; Paris *et al.*, 2009), impacts of the tsunami on natural environments (Hulugalle *et al.*, 2009; Irtem *et al.*, 2009; Violette *et al.*, 2009), and ecological protection mechanisms against tsunami damage (Kathiresan and Rajendran, 2005; Cochara *et al.*, 2008; Yanagisawa *et al.*, 2009; Kaplan *et al.*, 2009). The 2004 Indian Ocean tsunami was one of the largest and deadliest tsunamis in recorded human history, and Aceh Province in Sumatra suffered the highest human losses, with 163,978 people dead.

*Researcher, Dept. of Spatial Information Engineering, Pukyong National University, Busan 608-737, Korea (E-mail: sinaga387@gmail.com)

**Researcher, Dept. of Geography, Gadjah Mada University, Indonesia, Kutai Timur 75683, Kaltim, Indonesia (E-mail: gluedux@yahoo.com)

***Assistant Professor, Dept. of Spatial Information Engineering, Pukyong National University, Busan, 608-737, Korea (E-mail: modconfi@pknu.ac.kr)

****Member, Associate Professor, Dept. of Spatial Information Engineering, Pukyong National University, Busan 608-737, Korea (Corresponding Author, E-mail: suh@pknu.ac.kr)

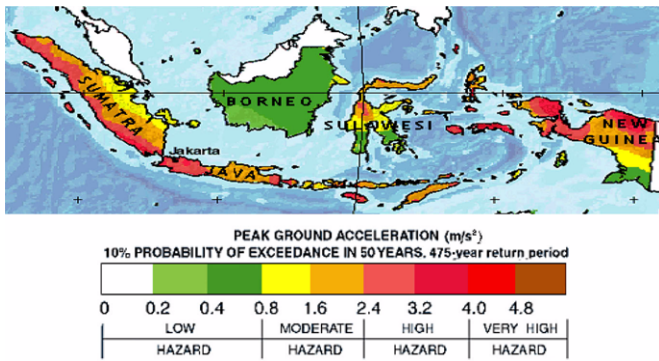


Fig. 1. Seismic Hazard Map of Indonesia (<http://geology.about.com/library/bl/maps/blindonesiasemap.htm>)

Our study area, the Jembrana Regency in Bali, was also struck by a tsunami with 4-m run-up caused by the 1994 Java earthquake of magnitude 7.2 (Abercrombie *et al.*, 2001; Diposaptono and Budiman, 2005). Jembrana directly faces the Indian Ocean, the junction site of the Eurasian, Australian, and Pacific tectonic plates. These plates are still stabilizing and have the possibility of colliding. The Bali Strait between the islands of Bali and Java also increases the risk of tsunami by narrowing the width of wave streak. Serious earthquakes have long been reported around this area, and similar events could happen in the future. Considering the above, estimation of tsunami vulnerability according to regional environmental characteristics can aid in the management and mitigation of potential disasters.

Recent studies have investigated tsunami vulnerability by analyzing multiple variables that can influence tsunami damage. Such studies have combined variables into a vulnerability index using a weighted mean (Papathoma *et al.*, 2003; Papathoma and Dominey-Howes, 2003; Dominey-Howes and Papathoma, 2006; Dominey-Howes *et al.*, 2009; Omira *et al.*, 2009), but in most cases, the weighting scheme was somewhat subjective and not based on scientific grounding. As an alternative, Dall’Osso *et al.* (2009) used the Analytic Hierarchy Process (AHP) as a more reasonable weighting method. However, their study focused on tsunami vulnerability at the small scale of individual buildings.

In this paper, we describe a GIS-based multi-criteria analysis of tsunami vulnerability for the Jembrana Regency in Bali, Indonesia. We used multiple geospatial variables such as topographic elevation and slope, topographic relation to tsunami direction, coastal proximity, and coastal shape. Whereas previous studies have analyzed the structural characteristics of buildings, we dealt with the regional environmental characteristics to create a continuous map of tsunami vulnerability on a 30-m grid. Furthermore, we utilized expert knowledge and employed the AHP method to create a weighting scheme for the geospatial variables. By overlaying an official land-use map on the tsunami vulnerability map, we could distinguish vulnerable areas in relation to land uses classified into 15 categories. Identification of tsunami-vulnerable areas can help in mitigating future natural disasters and reducing human and environmental damage.

This section has briefly introduced the background and objective of our study. In section 2, we describe the data processing and classification of geospatial variables that can be combined to estimate the degree of tsunami vulnerability. Section 3 presents our multi-criteria analysis of tsunami vulnerability in Jembrana using the geospatial variables and shows the spatial characteristics of tsunami vulnerability in relation to land-use types. In section 4, we summarize the study and discuss the implications and limitations of the work.

2. Geospatial Data Processing

2.1 Study Area

The Jembrana Regency is located between 114°25'53"-114°56'38" E longitude and 8°09'30"-8°28'02" S latitude, covering a total area of 841.9 km², and consisting of four sub-districts (Melaya, Negara, Mendoya, and Pekutan) and 83.3 km of coastline. Approximately 260,000 people live in the regency, with most residing in coastal areas. Climatically, the region experiences wet conditions from October to March and dry conditions between April and September. Temperature remains steady year round, with only slight decreases in the dry season. The monthly minimum temperature ranges between 23 and 26°C, and the monthly maximum temperature is 31 to 33°C. Monthly precipitation ranges from 100 to 300 mm in the wet season and less than 100 mm in the dry season. We choose the Jembrana Regency based on its history of tsunami occurrences, geophysical situation, and data availability.

2.2 Topographic Elevation

Topographic elevation is a primary condition to assess the tsunami vulnerability of a region. We used the Digital Elevation Model (DEM) from the Shuttle Radar Topography Mission (SRTM) to obtain the topographic elevations of the study area. The 90-m grid was downscaled to a 30-m grid using bilinear interpolation, and elevations were classified into five groups considering the tsunami run-up height at the coast (Iida, 1963). Table 1 and Fig. 2 show the vulnerability in terms of topographic elevation.

2.3 Topographic Slope

Topographic slope was calculated using the algorithm of Burrough and McDonnell (1998). The slope for a grid cell is given as $\sqrt{(\partial z/\partial x)^2 + (\partial z/\partial y)^2}$, where $\partial z/\partial x$ is the angle for east-

Table 1. Vulnerability in Terms of Topographic Elevation

Elevation (m)	Vulnerability
5 or lower	High
5–10	Rather high
10–15	Medium
15–20	Rather low
20 or higher	Low

(Source: Iida, 1963)

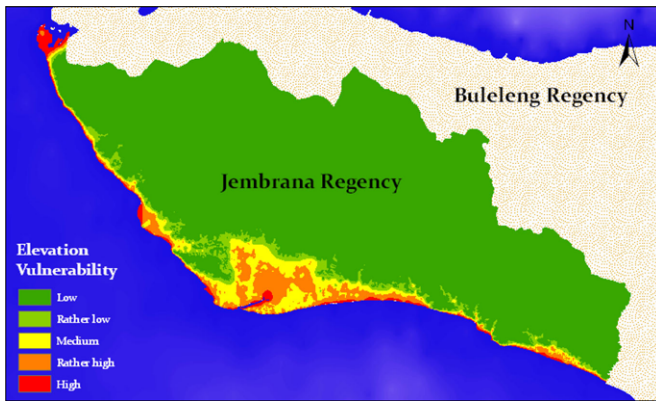


Fig. 2. Vulnerability Map of Jembrana in Terms of Topographic Elevation

west direction, and $\partial z/\partial y$ is the angle for north-south direction. Tsunami run-up can be severe in areas of relatively flat topographic slope because the tsunami can easily flow onto flat areas, but may be detained or deflected by hills bordering the beach. We employed the slope classification of Van Zuidam (1983). Table 2 and Fig. 3 show the vulnerability in terms of topographic slope.

2.4 Topographic Relation to Tsunami Direction

The direction of tsunami wave propagation will influence its speed and height at the coast. Areas lying perpendicular to the direction of a tsunami wave can be greatly affected by the energy

Table 2. Vulnerability in Terms of Topographic Slope

Topographic slope (%)	Vulnerability
0-2	High
2-6	Rather high
6-13	Medium
13-20	Rather low
20+	Low

(Source: Van Zuidam, 1983)

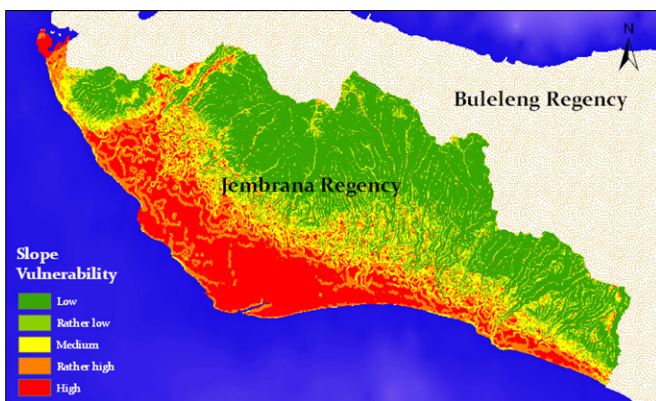


Fig. 3. Vulnerability Map of Jembrana in Terms of Topographic Slope

Table 3. Vulnerability in Terms of the Topographic Relation to Tsunami Direction

Topographic relation to tsunami direction	Vulnerability
Perpendicular	High
Oblique	Medium
Covered	Low

(Source: Diposaptono and Budiman, 2005)

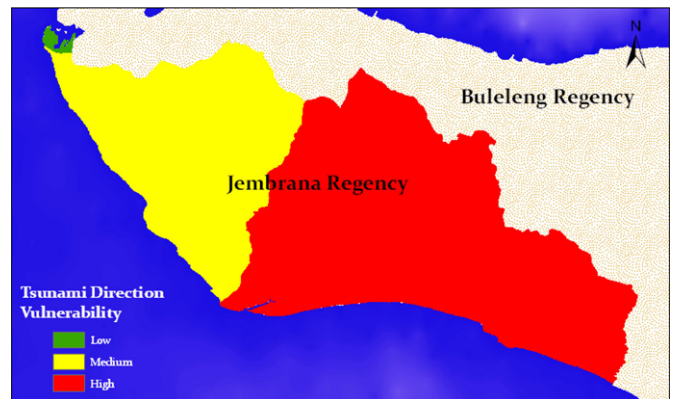


Fig. 4. Vulnerability Map of Jembrana in Terms of the Topographic Relation to Tsunami Direction

concentration of the wave (Diposaptono and Budiman, 2005; Umitu *et al.*, 2007). Areas covered (protected by other land features) from the direction of a tsunami wave may be protected from its reaches. Areas oblique to the direction of the tsunami wave may be subject to intermediate effects. We assigned values to each of these three categories, as shown in Table 3. One of the values was then assigned to each grid cell according to the geophysical aspects of the study area (Fig. 4).

2.5 Coastal Proximity

Using a vector map of the coastline, we calculated coastal proximity based on a 30-m grid. Distance from the coastline is associated with the possible reach of a tsunami. In general, vulnerability becomes higher as coastal proximity increases. To classify coastal proximity, we used the following equation from Bretschneider and Wybro (1976): $\log X_{max} = \log 1400 + 4/3 \log (Y_0/10)$, where X_{max} is the maximum reach of the tsunami over land, and Y_0 is the tsunami height at the coast. According to this formula, a tsunami with a 5-m run-up can reach up to 556 m from the shoreline. Run-up of 5 to 10 m can reach 556-1400 m from the shoreline, whereas run-ups of 10-15 and 15-20 correspond to distances of 1400-2404 m and 2404-3528 m, respectively, and so on. Vulnerability in terms of coastal proximity can be given as in Table 4. Fig. 5 shows the map of coastal proximity.

2.6 Coastal Shape

The coastline profile can also influence tsunami height and speed. Coasts with indentation may have higher run-ups than coasts without indentation because wave energy tends to

Table 4. Vulnerability in Terms of Coastal Proximity

Distance (m) from shoreline	Vulnerability
0-556	High
556-1400	Rather high
1400-2404	Medium
2404-3528	Rather low
3528+	Low

(Source: Bretschneider and Wybro, 1976)

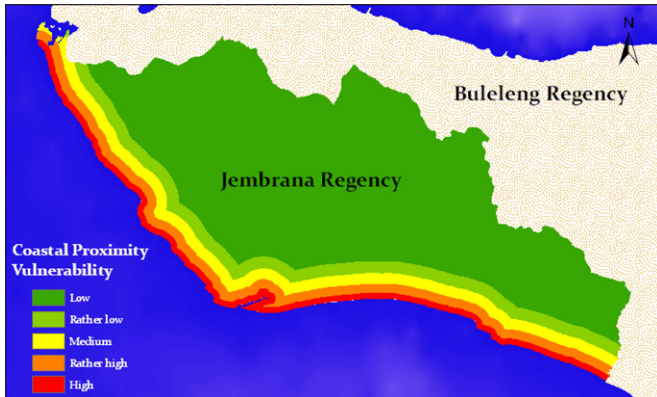


Fig. 5. Vulnerability Map of Jembrana in Terms of Coastal Proximity

concentrate within gulfs (Ikawati, 2004). We divided the study area into three categories: gulf, straight coast, and cape (Table 5), and assigned these categories to each grid cell by taking account of geophysical aspects of the study area (Fig. 6).

Table 5. Vulnerability in Terms of Coastal Shape

Coastal shape	Vulnerability
Gulf	High
Straight coast	Medium
Cape	Low

(Source: Ikawati, 2004)

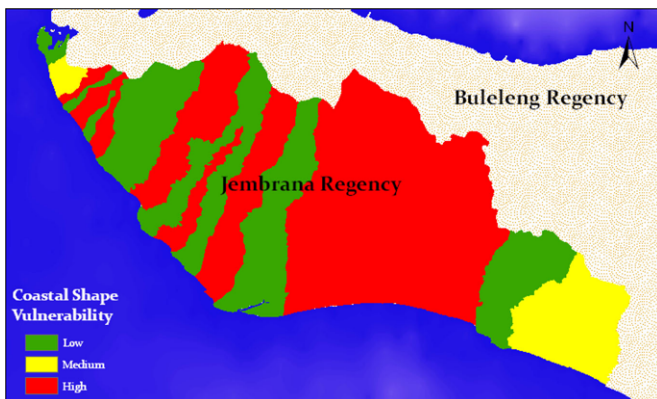


Fig. 6. Vulnerability Map of Jembrana in Terms of Coastal Shape

3. Multi-criteria Analysis and Vulnerability Mapping

3.1 Weighting Scheme

We used the five geospatial variables, namely topographic elevation and slope, topographic relation to tsunami direction, coastal proximity, and coastal shape, as the criteria for tsunami vulnerability. These variables were combined in the form of a weighed mean, and the weight for each variable was calculated using the AHP approach. The AHP is an effective method for eliciting expert knowledge and can be a useful tool for risk assessment of natural disasters, even if expert knowledge is often incomplete (Herath and Prato, 2006). Questionnaires regarding pair-wise comparisons between the five variables were completed by several environmental experts. The pair-wise comparison matrices were aggregated into a single matrix using the harmonic mean, and a normalized eigenvector was calculated for the weight of the five variables (Table 6).

Topographic elevation had the greatest weight because ground height is directly associated with tsunami inundation according to the run-up of tsunamis. The topographic relation to tsunami direction was considered to be more important than coastal proximity, because land lying perpendicular to the tsunami wave direction can be directly struck by the tsunami. Coastal shape and topographic slope had relatively low weights.

3.2 Tsunami Vulnerability Mapping

To integrate the five variables and derive the vulnerability index for Jembrana, we used a weighted mean of the variables in the form of $\sum_{i=1}^5 w_i s_i$, where w_i is the weight of the i th variable, and s_i is the score for the i th variable. Scores of 5, 4, 3, 2, and 1 were assigned to the categories “high,” “rather high,” “medium,” “rather low,” and “low,” respectively. Table 7 shows the resulting statistics of the tsunami vulnerability index, and Fig. 7 maps the index for the study area. The vulnerability values of approximately 900,000 grid cells ranged between 1.24 and 4.34, with a mean of 1.89 and a standard deviation of 0.60. We classified the

Table 6. Weights of the Five Geospatial Variables

Geospatial variable	Weight
Topographic elevation	0.414
Topographic slope	0.087
Topographic relation to tsunami direction	0.236
Coastal proximity	0.171
Coastal shape	0.092

Table 7. Statistics of Tsunami Vulnerability for Jembrana

Statistics	Value
Min	1.24
Max	4.34
Mean	1.89
Std. Dev.	0.60

Table 8. Classification of Tsunami Vulnerability

Vulnerability index	Class
1.24-1.70	Safe
1.70-2.10	Rather safe
2.10-2.75	Medium
2.75-3.43	Rather vulnerable
3.43-4.34	Vulnerable

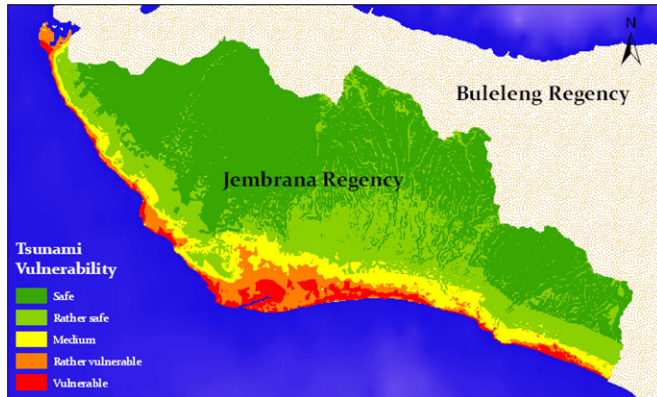


Fig. 7. Map of Tsunami Vulnerability for Jembrana

values into five groups (Table 8) using Jenks' natural break method, which minimizes the within-group Sum of Squared Difference (SSD) to make internally homogenous groups. In Jembrana, vulnerable and rather vulnerable areas were mostly found along the coast, and the southwest cape had a somewhat wide range of rather vulnerable areas, presumably because of its low elevation and coastline shape.

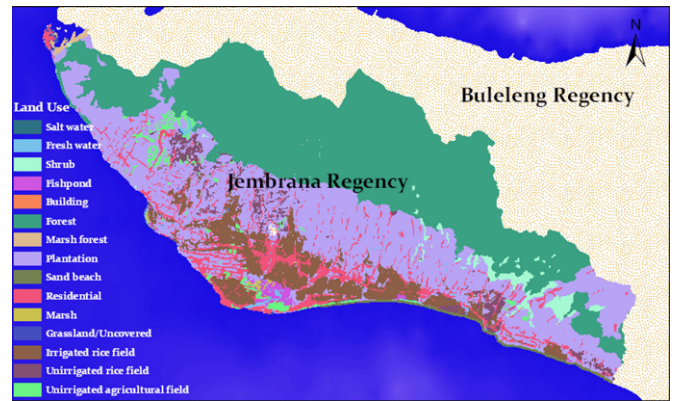


Fig. 8. Land use Classification for Jembrana

3.3 Comparisons with the Land-use Classification

In the Jembrana Regency, most of the population and valuable resources exist within coastal areas classified as vulnerable or rather vulnerable. To examine which types of land uses are at risk in more detail, we compared the land uses with the vulnerability map. Land-use information in Jembrana was obtained from the official land-use map provided by the National Coordinating Agency for Survey and Mapping, Indonesia (Fig. 8). The map contains 15 land-use classes including salt water, fresh water, shrub, fishpond, building, forest, marsh forest, plantation, sand beach, residential, marsh, grassland/uncovered, irrigated rice field, unirrigated rice field, and unirrigated agricultural field. Forest and plantation occupy about 75% of the Jembrana Regency, followed by agricultural and residential uses. Most buildings and residential areas are distributed close to the coast because of the flat topography and proximity to the sea.

Table 9. Overlay of the Land-use Classification and the Tsunami Vulnerability Map

	Area	Safe (%)	Rather safe (%)	Medium (%)	Rather vulnerable (%)	Vulnerable (%)	Sum (%)
Salt water	0.06 km ² (0.01%)	0.00	0.00	0.00	99.91	0.09	100
Fresh water	3.61 km ² (0.43%)	26.31	17.17	8.93	11.99	35.60	100
Shrub	16.37 km ² (1.94%)	73.09	25.65	0.55	0.49	0.21	100
Fishpond	5.32 km ² (0.63%)	0.00	0.00	0.00	26.62	73.38	100
Building	0.06 km ² (0.01%)	4.28	10.65	7.10	6.25	71.73	100
Forest	365.71 km ² (43.41%)	87.02	12.40	0.32	0.22	0.04	100
Marsh forest	1.50 km ² (0.18%)	0.00	0.00	2.23	90.34	7.43	100
Plantation	281.09 km ² (33.37%)	36.61	47.77	10.77	3.51	1.35	100
Sand beach	1.78 km ² (0.21%)	0.00	0.00	0.23	19.03	80.74	100
Residential	59.91 km ² (7.11%)	13.30	29.53	34.54	14.99	7.65	100
Marsh	1.02 km ² (0.12%)	0.00	0.00	0.05	52.22	47.73	100
Grassland/uncovered	1.46 km ² (0.17%)	13.26	1.45	4.93	46.05	34.31	100
Irrigated rice field	71.05 km ² (8.43%)	9.99	16.52	27.32	31.63	14.53	100
Unirrigated rice field	19.79 km ² (2.35%)	52.96	22.94	17.93	4.10	2.08	100
Unirrigated agricultural field	13.66 km ² (1.62%)	46.90	21.85	3.79	14.14	13.32	100
Sum	842.39 km ² (100%)	55.35	26.29	9.04	5.90	3.43	100

We overlaid the land-use classification on the tsunami vulnerability map (Table 9). Vulnerable or rather vulnerable areas make up 9.3% (78.6 km²) of Jembrana, whereas safe or rather safe areas cover 81.6% (687.7 km²). However, almost 80% of buildings and more than 20% of residential areas are in the vulnerable or rather vulnerable area, meaning that many people are at risk. Agriculture in Jembrana is also not safe because 46% of irrigated rice fields and 27% of unirrigated agricultural fields are located in the vulnerable or rather vulnerable area. Furthermore, fresh water is also at risk, and coastal ecosystems such as marshes may be affected by a tsunami, even though their total area is relatively small. As a result, tsunami occurrences around the Jembrana Regency have the potential to endanger human life, infrastructure, and the environment.

4. Conclusions

In this paper, we have described a multi-criteria analysis of tsunami vulnerability at a regional scale using geospatial variables within a GIS environment. We combined five geospatial variables (topographic elevation and slope, topographic relation to tsunami direction, coastal proximity, and coastal shape) using AHP and created a tsunami vulnerability map for the Jembrana Regency in Bali, Indonesia. Overlaying the land-use classification on the tsunami vulnerability map showed that buildings, residential, and agricultural areas are particularly at risk if a tsunami were to strike the study area.

GIS-based analyses can be useful in a wide range of disaster assessment, through the use of spatial functionalities such as topographic operations, proximity calculation, buffer creation, raster reclassification, map algebra, and intersection operations. Such approaches can aid in regional planning for management and mitigation of natural disasters, including tsunamis. However, such analyses can be limited by the availability of data necessary for estimating the risk of natural hazards. We used just five geospatial variables. More adequate environmental and socio-economic data will be required for better understanding of disaster occurrences and damages. Also, development of a more appropriate weighting scheme remains as a future work. Considering the tsunami catastrophes in Aceh and Pangandaran, we anticipate that tsunami vulnerability maps will contribute to preliminary mitigation and planning efforts in the Jembrana Regency.

Acknowledgements

This work was funded by the Korea Meteorological Administration Research and Development Program under Grant CATER 2009-3111.

References

Abercrombie, R., Antolik, M., Felzer, K., and Ekström, G. (2001). "The 1994 Java tsunami earthquake: Slip over a subducting seamount."

- Journal of Geophysical Research*, Vol. 106, No. B4, pp. 6595-6607.
- Bretschneider, C. L. and Wybro, P. G. (1976). "Tsunami inundation prediction." *Proceedings of the 15th ASCE Conference on Coastal Engineering*, pp. 1006-1024.
- Burrough, P. A. and McDonnell, R. A. (1998). *Principles of geographical information systems*, Oxford University Press, New York, p. 356.
- Cocharda, R., Ranamukhaarachchi, S. L., Shivakoti, G. P., Shipin, O. V., Edwards, P. J., and Seeland, K. T. (2008). "The 2004 tsunami in Aceh and Southern Thailand: A review on coastal ecosystems, wave hazards and vulnerability, perspectives in plant ecology." *Evolution and Systematics*, Vol. 10, No. 1, pp. 3-40.
- Dall'Osso, F., Gonella, M., Gabbianelli, G., Withycombe, G., and Dominey-Howes, D. (2009). "A revised (PTVA) model for assessing the vulnerability of buildings to tsunami damage." *Natural Hazards and Earth System Sciences*, Vol. 9, No. 5, pp. 1557-1565.
- Diposaptono, S. and Budiman, D. (2005). *Tsunami: Scientific popular book*, Bogor, Indonesia, p. 125.
- Dominey-Howes, D., Dunbar, P., Varner, J., and Papathoma-Köhle, M. (2009). "Estimating probable maximum loss from a Cascadia tsunami." *Natural Hazards*, Vol. 53, No. 1, pp. 43-61.
- Dominey-Howes, D. and Papathoma, M. (2007). "Validating a tsunami vulnerability assessment model (the PTVA model) using field data from the 2004 Indian Ocean tsunami." *Natural Hazards*, Vol. 40, No. 1, pp. 113-136.
- Fagherazzi, S. and Du, X. (2008). "Tsunamigenic incisions produced by the December 2004 earthquake along the coasts of Thailand, Indonesia and Sri Lanka." *Geomorphology*, Vol. 99, Nos. 1-4, pp. 120-129.
- Herath, G. and Prato, T. (2006). *Using multi-criteria decision analysis in natural resource management*, Ashgate Publishing, Surrey, UK, p. 239.
- Hulugalle, N. R., Jaya, R., Luther, G. C., Ferizal, M., Daud, S., Yatiman, Irhas, Yufniati, Z. A., Feriyanti, F., Tamrin, and Han, B. (2009). "Physical properties of tsunami-affected soils in Aceh, Indonesia: 2½ years after the tsunami." *CATENA*, Vol. 77, No. 3, pp. 224-231.
- Iida, K. (1963). "Magnitude, energy and generation mechanisms of tsunamis and a catalogue of earthquakes associated with tsunamis." *Proceedings of Tsunami Meeting at the 10th Pacific Science Congress*, pp. 7-18.
- Ikawati, Y. (2004) *Tsunami wave is predictable*, In Canahar, P., Earthquake Disaster and Tsunami, Kompas, Jakarta, Indonesia, p. 550.
- Irtem, E., Gedik, N., Kabdasli, M. S., and Yas, N. E. (2009). "Coastal forest effects on tsunami run-up heights." *Ocean Engineering*, Vol. 36, Nos. 3-4, pp. 313-320.
- Jaffe, B. E. and Gelfenbuam, G. (2009). "A simple model for calculating tsunami flow speed from tsunami deposits." *Sedimentary Geology*, Vol. 200, Nos. 3-4, pp. 347-361.
- Kaplan, M., Renaud, F. G., and Lüchters, G. (2009). "Vulnerability assessment and protective effects of coastal vegetation during the 2004 Tsunami in Sri Lanka." *Natural Hazards and Earth System Sciences*, Vol. 9, No. 4, pp. 1479-1494.
- Kathiresan, K. and Rajendran, N. (2005). "Coastal mangrove forests mitigated tsunami." *Estuarine, Coastal and Shelf Science*, Vol. 65, No. 3, pp. 601-606.
- Koh, H. L., Teh, S. Y., Liu, P. L.-F., Ismail, A. I. M., and Lee, H. L. (2009) "Simulation of Andaman 2004 tsunami for assessing impact on Malaysia." *Journal of Asian Earth Sciences*, Vol. 36, No. 1, pp. 74-83.

- Omira, R., Baptista, M. A., Miranda, J. M., Toto, E., Catita C., and Catalão, J. (2009). "Tsunami vulnerability assessment of Casablanca-Morocco using numerical modelling and GIS tools." *Natural Hazards*, Vol. 54, No. 1, pp. 75-95.
- Papathoma, M. and Dominey-Howes, D. (2003). "Tsunami vulnerability assessment and its implications for coastal hazard analysis and disaster management planning, Gulf of Corinth, Greece." *Natural Hazards and Earth System Sciences*, Vol. 3, No. 6, pp. 733-747.
- Papathoma, M., Dominey-Howes, D., Zong, Y., and Smith, D. (2003). "Assessing tsunami vulnerability, an example from Herakleio, Crete." *Natural Hazards and Earth System Sciences*, Vol. 3, No. 5, pp. 377-389.
- Paris, R., Lavigne, F., Wassmer, P., and Sartohadi, J. (2007). "Coastal sedimentation associated with the December 26, 2004 tsunami in Lhok Nga, west Banda Aceh (Sumatra, Indonesia)." *Marine Geology*, Vol. 238, Nos. 1-4, pp. 93-106.
- Paris, R., Wassmer, P., Sartohadi, J., Lavigne, F., Barthelemy, B., Desgages, E., Grancher, D., Baumert, P., Vautier, F., Brunstein, D., and Gomez, C. (2009). "Tsunamis as geomorphic crises: Lessons from the December 26, 2004 tsunami in Lhok Nga, West Banda Aceh (Sumatra, Indonesia)." *Geomorphology*, Vol. 104, Nos. 1-2, pp. 59-72.
- Roy, G. D., Karim, M. F., and Ismail, A. I. M. (2007). "A nonlinear polar coordinate shallow water model for tsunami computation along North Sumatra and Penang Island." *Continental Shelf Research*, Vol. 27, No. 2, pp. 245-257.
- Srinivasalu, S., Thangadurai, N., Switzer, A. D., Mohan, V. R., and Ayyamperumal, T. (2007). "Erosion and sedimentation in Kalpakkam (N Tamil Nadu, India) from the 26th December 2004 tsunami." *Marine Geology*, Vol. 240, Nos. 1-4, pp. 65-75.
- Umitsu, M., Tanavud, C., and Patanakanog, B. (2007). "Effects of landforms on tsunami flow in the plains of Banda Aceh, Indonesia, and Nam Khem, Thailand." *Marine Geology*, Vol. 242, Nos. 1-3, pp. 141-153.
- United Nations Environment Programme World Conservation Monitoring Centre (2009). In the front line: Shoreline protection and other ecosystem services from mangroves and coral reefs, available at http://www.unep.org/pdf/infrontline_06.pdf
- Van Zuidam, R. A. (1983) *Guide to geomorphologic - Aerial photographic interpretation and mapping*, International Institute for Geo-Information Science and Earth Observation, Enschede, The Netherlands, p. 325.
- Violette, S., Boulicot, G., and Gorelick, S. M. (2009). "Tsunami-induced groundwater salinization in southeastern India." *Comptes Rendus Geosciences*, Vol. 341, No. 4, pp. 339-346.
- Wijetunge, J. J. (2009). "Field measurements and numerical simulations of the 2004 tsunami impact on the south coast of Sri Lanka." *Ocean Engineering*, Vol. 36, Nos. 12-13, pp. 960-973.
- Yan, Z. and Tang, D. (2009). "Changes in suspended sediments associated with 2004 Indian Ocean tsunami." *Advances in Space Research*, Vol. 43, No. 1, pp. 89-95.
- Yanagisawa, H., Koshimura, S., Goto, K., Miyagi, T., Imamura, F., Ruangrassamee, A., and Tanavud, C. (2009). "The reduction effects of mangrove forest on a tsunami based on field surveys at Pakarang Cape, Thailand and numerical analysis." *Estuarine, Coastal and Shelf Science*, Vol. 81, No. 1, pp. 27-37.